Research Article | Vol. 28, No. 26 / 21 December 2020 / Optics Express 39841
Optics EXPRESS

Dynamically tunable transmissive color filters using ultra-thin phase change materials

QIANG HE,[1,2] NATHAN YOUNGBLOOD,[1,3,5] ZENGGUANG CHENG,[1,4] XIANGSHUI MIAO,[2] AND HARISH BHASKARAN[1,6]

[1]Department of Materials, University of Oxford, Parks Road, Oxford OX13PH, UK
[2]Wuhan National Research Center for Optoelectronics, School of Optical and Electronic Information, Huazhong University of Science and Technology, Wuhan 430074, China
[3]Present address: Department of Electrical and Computer Engineering, Swanson School of Engineering, University of Pittsburgh, Pittsburgh, PA 15261, USA
[4]Present address: State Key Laboratory of ASIC and System, School of Microelectronics, Fudan University, Shanghai 200433, China
[5]nathan.youngblood@upitt.edu
[6]harish.bhaskaran@materials.ox.ac.uk

Abstract: Structural color filters (i.e. plasmonics and nano-cavities) provide vivid and robust color filtering in applications such as CMOS image sensors but lack simplicity in fabrication and dynamic tuning. Here we report a dynamically tunable, transmissive color filter by incorporating an ultra-thin phase change layer inside a thin-film optical resonator. The transmitted color spectrum can be designed over the entire visible range and shifted by around 50 nm after phase transition. Angle dependence shows little color variation within a ±30° viewing angle. Crucially, only film deposition is required to fabricate our phase change color filter, showing great potential for large-scale and inexpensive production. The dynamically tunable color filter, described in this paper, could be a promising component in display, CMOS sensor, and solar cell technology.

1. Introduction

Color filters (CFs), either transmissive or reflective, have been regarded as vital components in CMOS image sensors, smart windows, solar-cells and nano-display applications [1–4]. Colorant pigments, which were widely used as the key-technology for producing on-chip color filters [3], are currently limited by the process cost, resolution and color durability requirements. Structural color filters, based on the interaction between light and nanostructures rather than material properties, have been extensively demonstrated and still intrigue researchers in science and engineering [5–10]. The color response of these devices is controlled by manipulating the resonance in plasmonics and MIM (metal-insulator-metal) nanostructures, which reduce cost and provide better color purity, higher resistance to the chemicals and heat. Furthermore, dynamically modulating color has long been a scientific "dream", since it promises simplified fabricating process, ultra-high resolution and a reconfigurable color display. However, the wideband dynamic tuning of the transmissive light across the entire visible spectrum remains challenging, although recent progresses have been obtained in the active reflective display featuring low energy operation and high resolution by our previous work [11,12] and others [13,14].

Phase change materials (PCMs), which have been traditionally used in DVDs and solid-state electronic storage [15–17], recently attract much attention for optical tuning across visible and near-infrared (NIR) range exploiting either metasurface or nano-cavity structures [18–21]. Spectrally-tunable Fabry-Perot bandpass filters operating across the mid-infrared have been demonstrated by utilizing PCMs [19,20], but little work has been done on tunable transmissive

#411874 https://doi.org/10.1364/OE.411874
Journal © 2020 Received 12 Oct 2020; revised 18 Nov 2020; accepted 24 Nov 2020; published 16 Dec 2020

Optics EXPRESS

filters at visible wavelengths using these materials. Because PCMs, such as $Ge_2Sb_2Te_5$ (GST), can be reversibly switched between bistable states at nanosecond time scales under optical or electrical excitation, they serve as active optical materials, which provide dynamic modulation of optical properties [22]. Previous work has shown the first GST-based reflective display device utilizing an optoelectronic framework with low-dimensional phase change layer [11], enabling higher resolution, faster switching and lower power consumption. Additionally, ultra-fast phase change absorbers working at NIR range have been demonstrated for applications such as thermal emitters and photodetectors [23]. Similarly, active optical tuning of transmitted light in the NIR has also been implemented by combining PCMs with plasmonic, which show potential in smart window and telecommunication applications [21]. However, dynamically tunable transmissive color filters based on phase change materials have so far not been demonstrated. Such filters are potentially useful for creating active pixels for imaging devices such as CMOS image sensors, which can be readily modulated across the entire visible wavelength at high speeds.

In this work, we present a lithography free active color filter based on a incorporating a phase change material within an optical cavity. A thin-film optical cavity based on Fabry-Pérot resonances produces strong, vivid color selection due to the interference of the waves in the multilayer structure. $Ge_2Sb_2Te_5$ (GST) is used as the dynamic optical material to modulate the transmitted color. The transmittance can be continuously tuned across the visible spectrum by adjusting the thicknesses of the dielectric layers within the cavity. Furthermore, our color filters do not require any complicated lithographic methods during fabrication, which greatly reduces the cost and complexity of our device.

2. Results and discussion

A schematic of the proposed device is shown in Fig. 1(a). The color filters, which consist of a resonant cavity covered by an optimized anti-reflection coating (ARC), are designed on a transparent glass substrate. Silver (Ag) film was used as semi-transparent mirrors in our work, since it features relatively low optical absorption and high reflectivity in the visible spectrum. GST acts as the active optical material here, due to its significant optical properties between amorphous and crystalline states. The dielectric inter-cavity spacer and ARC was composed of Silicon dioxide (SiO_2) since it exhibits low loss and a relatively uniform refractive index in the visible.

Since the wavelength-dependent interference and absorption in the multilayer structure strongly depends on the dielectric thickness within the cavity, we varied the thicknesses of both spacer layers to obtain a full palette of colors that span the visible range. The thickness of Ag mirrors was fixed at 20 nm which gave a good trade-off between maximizing both optical transmission and color fidelity (see Supplement 1, Fig. S1) and minimizing losses due to discontinuities in the deposited film [24]. A SiO_2 ARC of 94 nm was optimized for suppressing reflection and protecting the top Ag layer from being oxidized. Because thick GST dramatically reduces the intensity of transmission without improving color modulation, a 7 nm-thick phase change layer was used, which is also the minimum thickness we could reliably sputter using our deposition system. A comparison of calculated color arrays at crystalline and amorphous states is shown in Fig. 1(b). The simulation was based on the standard transfer matrix method (TMM) [25]using experimentally measured refractive indexes from our materials. The TMM approach simplifies multi-layer optical stacks to a series of interface and propagation matrices that define the complex reflection, transmission, and phase accumulation of the optical field as it propagates through the layers. The interface and propagation matrices (I_{jk} and L_j, respectively) are defined as:

$$I_{jk} = \frac{1}{t_{jk}} \begin{bmatrix} 1 & r_{jk} \\ r_{jk} & 1 \end{bmatrix}, \quad L_j = \begin{bmatrix} e^{-ik_j d_j} & 0 \\ 0 & e^{ik_j d_j} \end{bmatrix} \tag{1}$$

Optics EXPRESS

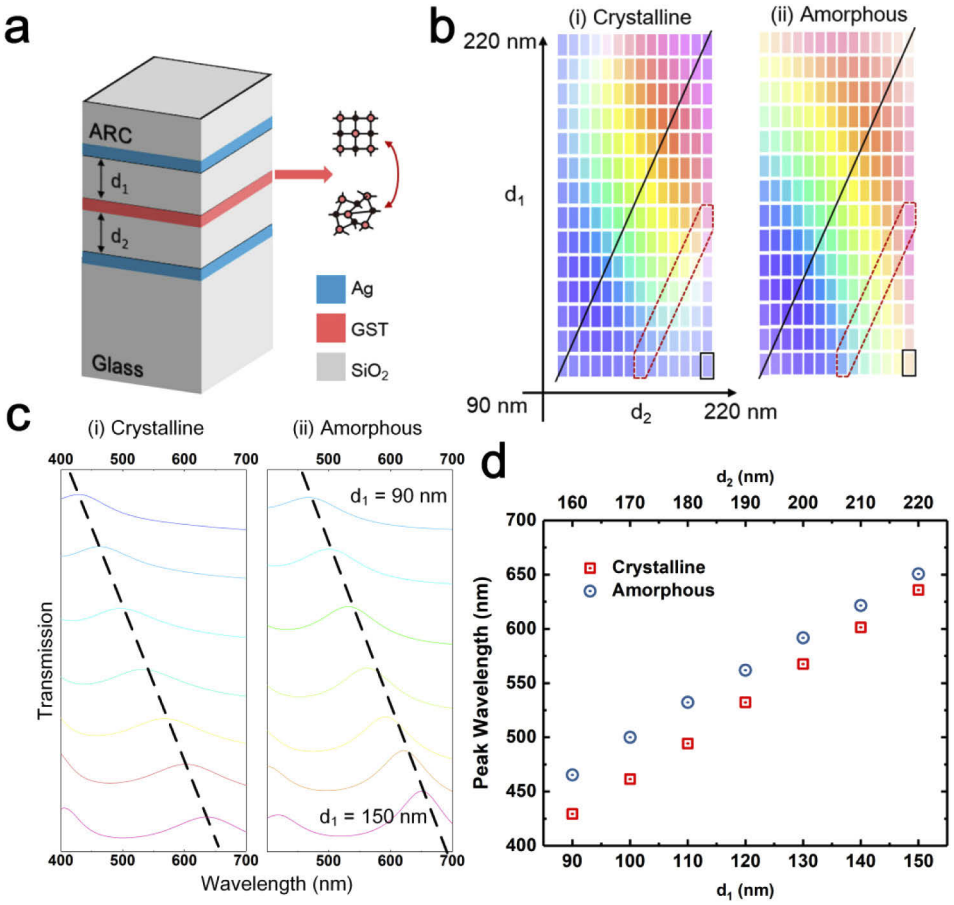

Fig. 1. a) Schematic of the proposed dynamic color filter based on phase change material and optical cavity structure. A phase transition between the amorphous and crystalline states occurs via heating. b) By modifying the inter-cavity thicknesses, tuning over the visible spectrum is possible. The full palette is also shifted after a phase transition of the GST layer. c) Selected spectra of crystalline and amorphous states shows the color tunability provided by phase change material. The dashed lines mark the peak movements of varying cavity sizes at different states. d) Peak wavelength shifts extracted from c) illustrate the color modulation due to the phase transition.

Optics EXPRESS

Here, r_{jk} and t_{jk} are the complex Fresnel reflection and transmission coefficients defined as (for the case of normal incidence):

$$r_{jk} = \frac{\tilde{n}_j - \tilde{n}_k}{\tilde{n}_j + \tilde{n}_k}, \quad t_{jk} = \frac{2\tilde{n}_j}{\tilde{n}_j + \tilde{n}_k} \tag{2}$$

where $\tilde{n}_j$ is the complex refractive index of the j^{th} layer. The layer phase thickness ($k_j d_j = (2\pi n_j/\lambda)d_j$, is the optical thickness of the light as it propagates through the j^{th} layer of the multi-layer stack. Combining multiple interface and propagation matrices together provides a computationally simple method for accurately calculating the total transmission, reflection, and absorption of the optical stack.

For both crystalline and amorphous GST-based color filters, transmitted color is produced and continuously tuned in the visible spectrum by adjusting the inter-cavity SiO_2 thicknesses. As the thickness of both SiO_2 layers are increased from 90 nm to 220 nm, the color is gradually tuned from blue to red. Additionally, the PCM enables the color to be modulated once the cavity design is fixed. By varying the SiO_2 layer thicknesses, we classify the proposed CFs into two categories: symmetrical ($d_1 = d_2$) and asymmetrical ($d_1 \neq d_2$) color filters. For the asymmetrical color filters, the greater difference between cavities reveals the more significant color contrast before and after phase change of GST. For instance, the transmitted color is tunable between blue and orange, when $d_1 = 90$ nm and $d_2 = 220$ nm (as depicted in the black boxes). However, in the symmetrical CF simulations, the color remains nearly unchanged if the SiO_2 layers both have the same thickness (black solid line), as also shown in Supplement 1, Fig. S2.

In order to dynamically tune the color within the visible band while maintaining high color contrast between the amorphous and crystalline states, we present the transmission spectra at normal incidence for a cavity with d_2 - $d_1 = 70$ nm (indicated by the red dashed boxes in Fig. 1(b)). As shown in Fig. 1(c), each transmission spectra shows a peak which shifts to longer wavelengths with an increasing cavity thickness. The simulations also show that the transmission peak undergoes a blue-shift once the amorphous GST layer is crystallized. Figure 1(d) compares the peak shift resulting from phase transition at different cavity configurations. The maximum peak shift is approximately 50 nm when $d_1 = 90$ nm and $d_2 = 160$ nm. As the cavity thickness increases, the effect of the PCM's phase transition on the peak shift gradually decreases.

From Fig. 1(b), we see that there is an apparent design trade-off with our device paradigm between tunability and spectral purity. For large differences between d_1 and d_2 (see top left and bottom right color boxes in Fig. 1(b)), a the maximum spectral tunability due to a phase change can be observed (i.e. a phase transition in GST causes the transmitted color to switch between blue and red). However, these colors are less vivid and defined compared to designs where d_1 and d_2 are of similar size. This is due to the fact that as the GST layer is moved closer to the maximum field intensity within the FP resonator, both the light-matter interaction and optical losses increase which in turn maximize the tunability and reduce the spectral definition of the transmitted light. In our experimental demonstration below, we have sought to balance these trade-offs by reducing the tuning range between blue and green which improves spectral definition.

As creating the primary colors (blue, green and red) is crucial for CMOS image sensor and display applications, we now experimentally demonstrate a tunable blue/green color filter. Using the above simulations as a guide, the inter-cavity spacers, d_1 and d_2, were chosen to be 110 nm and 180 nm respectively. Figure 2(a) shows the resulting transmitted color of amorphous and crystalline color filter stacks. The PCM is known to be in the amorphous state as sputtered resulting in a green color, while PCM in the crystalline state results in blue. To fully crystalize the GST layer, we heat the as-fabricated amorphous sample to 225 °C for 15 minutes on a hot plate, although the phase transition is known to occur at much higher speeds [26,27]. Figure 2(b) presents a comparison between the measured and simulated transmission spectra with white

Optics EXPRESS

light illumination for the blue (crystalline) and green (amorphous) color filters. The measured transmission peak positions agree well with the calculated peaks that appear at 488 nm and 531 nm for crystalline and amorphous CFs, respectively. The peak shift before and after crystallization is therefore significant enough for obtaining tunable blue/green color filters. On the other hand, the transmission spectra of both the crystalline and amorphous CFs show only one resonance peak in the visible, which reveals the high color purity of fabricated CF samples. To demonstrate the color selectivity and high transmission of our filters, optical images with and without the CFs are shown in Fig. 2(c). Here, the scenery background, imaged with a CF and camera, are clearly seen with distinctive blue and green.

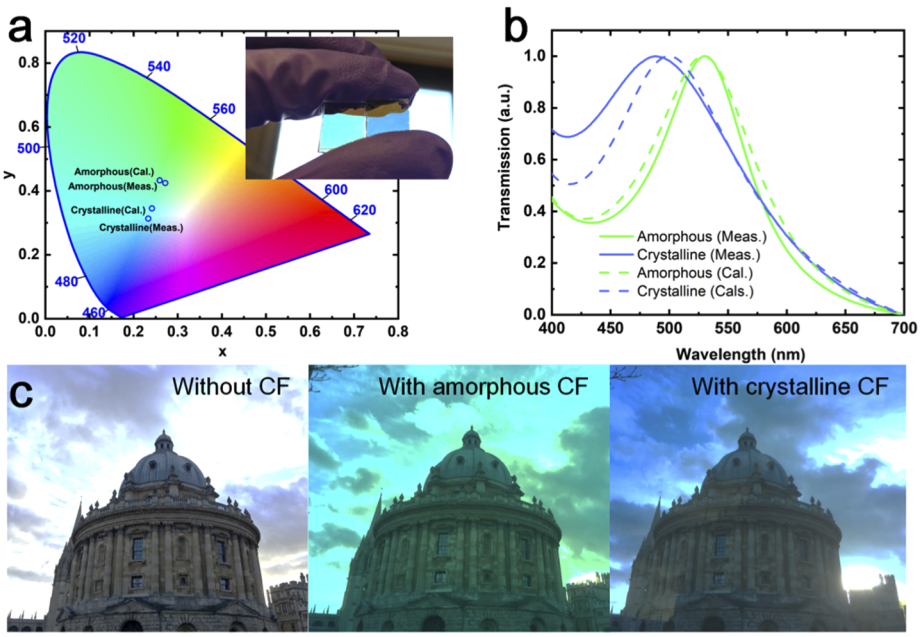

Fig. 2. a) CIE diagram and optical image of fabricated blue/green color filters. The green (left) is as-fabricated sample (amorphous), while the blue sample is in the crystalline state after baking. b) Experimental (solid lines) and simulation (dashed lines) spectra of the fabricated samples. c) Optical images of the Radcliffe Camera taken without CF, with amorphous CF, and with crystalline CF (from left to right).

To better understand the mechanism that governs the color modulation in our CFs, we plot the simulated electric filed distributions (shown in Fig. 3(a)) of our fabricated color filter in both states. The refractive index of GST used in the simulation has been experimentally measured and plotted in Fig. 3(b). Firstly, E-field distribution of a duplicate of our fabricated CF with no GST is simulated as a reference. The simulation with no GST shows that the Ag/SiO_2/Ag layers form an FP resonator. At resonance frequency 515 nm, the standing wave appears two loops with one node in the middle. Subsequently, the optical response is manipulated by inserting a thin layer of phase change materials inside the SiO_2. The simulation of amorphous GST indicates the phase change layer changes the cavity resonance through a phase shift and change in absorption. Additionally, the resonance peak is blue-shifted by crystallization, since the phase change material features different optical properties between crystalline and amorphous. The simulation in Fig. 3(a) also explains that putting the phase change layer in the center of the symmetric cavity (i.e. the wave node) doesn't contribute too much to the color change. To evaluate the tunability provided by phase change layer, Fig. 3(b) calculates the absorbance in the

Optics EXPRESS

GST layer. The phase change layer absorbs more light in the amorphous state than the crystalline state for wavelengths less than 441 nm, allowing higher transmission for colors in the blue-region of the visible spectrum. On the other hand, more light is absorbed by crystalline GST between 441 nm and 527 nm wavelengths, absorbing a greater portion of the green-region of the visible spectrum. Such an anamolous absorption behavior due to the cavity design has been reported earlier [28], and this explains why the transmitted color is blue and green when the proposed color filter is at crystalline and amorphous states, respectively.

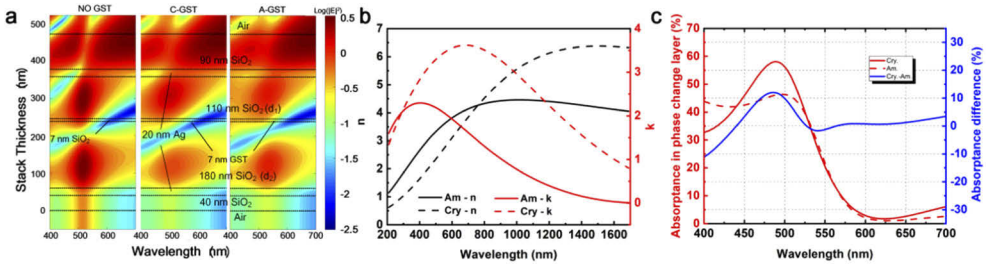

Fig. 3. a) Calculated electric field intensity profiles of the fabricated optical stack at no GST, amorphous and crystalline states. b) The refractive index of GST at both states used in the simulation. c) Optical absorption in the phase change layer in both amorphous and crystalline states (left axis) and the absorption difference as a function of wavelength (right axis).

We now move on to investigating the angle tolerance of our optical stack which is a key consideration in color filter design. The viewing angle dependence of the green color filter was demonstrated experimentally, as illustrated in Fig. 4(a). A logo was printed on white paper, illuminated from behind with a white light source, and filtered by the green CF shown in Fig. 2. Figure 4(b) compares the optical images taken at different viewing angles up to 45°. The transmitted pattern shows a slight color variation between the viewing angles of 0° and 30°, but shifts to blue when the angle increases to 45°. The angle resolved transmission spectra of the green CF (amorphous) for unpolarized incident light are shown in Fig. 4(c). The experimental results provide good qualitative agreement with simulation, both showing a blue-shifted transmission peak with increasing incident angle. Although the filtered color shows faint color variation before 30° incident angle, the angle tolerance could be continuously improved by incorporating angle-insensitive designs [8,29,30].

By employing phase change materials, we show that a solid-state, tunable color filter can be developed with a simple thin-film optical stack. Since phase change materials are switched thermally, an active color filter with selectable pixels in a color filter array (CFA) could be controlled either electrically or optically which would dramatically reduce the process cost of existing CFA fabrication. Thermally switched pixels have been demonstrated before and such a system would be compatible with our CFs [31,32]. In current metal-insulator-metal CFAs, individual lithography and film deposition process are used for the fabrication of each pixel's fixed color (i.e. blue, green and red) [1]. Utilizing phase change color filters, all the pixels could be deposited in a uniform thin-film and later configured to a certain CFA using electrical or optical pulses. Additionally, a phase change CF makes it possible to switch between different standard CFA at the same physical location, such as between a Bayer and CYGM color filter array. To achieve this, conductive transparent material, such as ITO (Indium Tin Oxide) could be chosen to replace SiO_2 within the resonator. Compared with plasmonic color filters, the multilayer structure investigated in this work is a lithography-free method, which is simpler and less costly to fabricate.

Optics EXPRESS

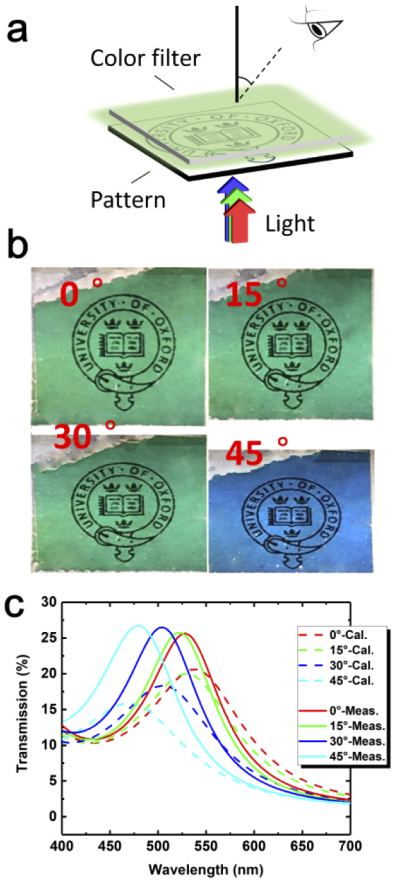

Fig. 4. a) Illustration of angular dependence experiment for images shown in b). White light passes though patterned paper and is filtered by the green color filter. Transmitted color varies as a function of observation angle. b) Optical images of filtered Oxford University logo taken at various observation angles. The size of fabricated sample is 1.2 cm × 1.2 cm. c) Measured and calculated transmission spectra of the fabricated green color filter device from the normal incidence to oblique incidence angles of 15°, 30° and 45°.

3. Conclusion

To summarize, a novel method to produce dynamically tunable color filters is proposed and verified experimentally. We have demonstrated the design of transmissive optical filters that can be fabricated to cover a given tuning range within the visible spectrum by manipulating the thicknesses of the SiO_2 layers within the cavity. A binary blue/green CF was fabricated and characterized, revealing that the absorbance difference between two states of PCM resulting from the phase transition shifts the resonance of the cavity. The angle dependent performance confirms that the fabricated color filter exhibits low angular sensitivity within the range of 0° to 30°. The transmission efficiency may be further enhanced by including an anti-reflection thin-film coating in the stack design in addition to reducing the absorption of GST in the amorphous state. Overall, the proposed phase change color filter has a diverse range of possible applications, such as CMOS sensors, OLED displays and solar cells.

Optics EXPRESS

4. Experimental section

Device fabrication: GST layers in our color filter devices were deposited using a Nordiko sputtering tool, while the Ag and SiO_2 layers were coated by electron-beam evaporation. To protect the sample from oxidation, a 7 nm SiO_2 capping layer was sputtered in-situ after the GST layer was deposited before transferring the samples to the evaporator for the remaining deposition.

Optical characterization: A PerkinElmer Lamda 1050 Spectrometer was used to characterize the spectral transmittance curves at different incident angles. All spectra were normalized to a background spectrum containing a blank SiO2 substrate.

Funding

China Scholarship Council (201600160015); Engineering and Physical Sciences Research Council (EP/J018694/1, EP/M015173/1, EP/M015130/1).

Acknowledgements

We acknowledge the financial support from EPSRC via grants EP/J018694/1, EP/M015173/1, and EP/M015130/1 in the UK. Q. H. also would like to thank the partial support from China Scholarship Council (CSC) (201600160015).

Disclosures

The authors declare no conflicts of interest.

See Supplement 1 for supporting content.

References

1. L. Frey, P. Parrein, J. Raby, C. Pellé, D. Hérault, M. Marty, and J. Michailos, "Color filters including infrared cut-off integrated on CMOS image sensor," Opt. Express **19**(14), 13073–13080 (2011).
2. K. Kumar, H. Duan, R. S. Hegde, S. C. Koh, J. N. Wei, and J. K. Yang, "Printing colour at the optical diffraction limit," Nat. Nanotechnol. **7**(9), 557–561 (2012).
3. H. Taguchi and M. Enokido, "Technology of color filter materials for image sensor," Red **10502**(8892), 3216 (2017).
4. H. J. Park, T. Xu, J. Y. Lee, A. Ledbetter, and L. J. Guo, "Photonic color filters integrated with organic solar cells for energy harvesting," ACS Nano **5**(9), 7055–7060 (2011).
5. D. Mazulquim, K.J. Lee, L.V. Muniz, B.-H.V. Borges, L.G. Neto, and R. Magnusson, "High Selectivity Plasmonic Color Filter Using a Single Dielectric Film Layer," In *Frontiers in Optics* pp. FTh3D. 7, (2014).
6. V. Vashistha, G. Vaidya, P. Gruszecki, A. E. Serebryannikov, and M. Krawczyk, "Polarization tunable all-dielectric color filter based on cross-shaped Si nanoantennas," Sci. Rep. **7**(1), 8092 (2017).
7. J. Wang, Q. Fan, S. Zhang, Z. Zhang, H. Zhang, Y. Liang, X. Cao, and T. Xu, "Ultra-thin plasmonic color filters incorporating free-standing resonant membrane waveguides with high transmission efficiency," Appl. Phys. Lett. **110**(3), 031110 (2017).
8. C. Yang, W. Shen, Y. Zhang, K. Li, X. Fang, X. Zhang, and X. Liu, "Compact multilayer film structure for angle insensitive color filtering," Sci. Rep. **5**(1), 9285 (2015).
9. F. Ye, M. J. Burns, and M. J. Naughton, "Structured metal thin film as an asymmetric color filter: the forward and reverse plasmonic halos," Sci. Rep. **4**(1), 7267 (2015).
10. Y. Yu, L. Wen, S. Song, and Q. Chen, "Transmissive/reflective structural color filters: theory and applications," J. Nanomater. **2014**, 1–17 (2014).
11. P. Hosseini, C. D. Wright, and H. Bhaskaran, "An optoelectronic framework enabled by low-dimensional phase-change films," Nature **511**(7508), 206–211 (2014).
12. C. Ríos, P. Hosseini, R. A. Taylor, and H. Bhaskaran, "Color Depth Modulation and Resolution in Phase-Change Material Nanodisplays," Adv. Mater. **28**(23), 4720–4726 (2016).
13. C. H. Park, Y. T. Yoon, V. R. Shrestha, C. S. Park, S. S. Lee, and E. S. Kim, "Electrically tunable color filter based on a polarization-tailored nano-photonic dichroic resonator featuring an asymmetric subwavelength grating," Opt. Express **21**(23), 28783–28793 (2013).

Optics EXPRESS

14. M. L. Tseng, J. Yang, M. Semmlinger, C. Zhang, P. Nordlander, and N. J. Halas, "Two-Dimensional Active Tuning of an Aluminum Plasmonic Array for Full-Spectrum Response," Nano Lett. **17**(10), 6034–6039 (2017).
15. S. G. Sarwat, P. Gehring, G. Rodriguez Hernandez, J. H. Warner, G. A. D. Briggs, J. A. Mol, and H. Bhaskaran, "Scaling limits of graphene nanoelectrodes," Nano Lett. **17**(6), 3688–3693 (2017).
16. M. H. Lankhorst, B. W. Ketelaars, and R. A. Wolters, "Low-cost and nanoscale non-volatile memory concept for future silicon chips," Nat. Mater. **4**(4), 347–352 (2005).
17. A. V. Kolobov, P. Fons, A. I. Frenkel, A. L. Ankudinov, J. Tominaga, and T. Uruga, "Understanding the phase-change mechanism of rewritable optical media," Nat. Mater. **3**(10), 703–708 (2004).
18. F. F. Schlich, P. Zalden, A. M. Lindenberg, and R. Spolenak, "Color Switching with Enhanced Optical Contrast in Ultrathin Phase-Change Materials and Semiconductors Induced by Femtosecond Laser Pulses," ACS Photonics **2**(2), 178–182 (2015).
19. M. N. Julian, C. Williams, S. Borg, S. Bartram, and H. J. Kim, "Reversible optical tuning of GeSbTe phase-change metasurface spectral filters for mid-wave infrared imaging," Optica **7**(7), 746–754 (2020).
20. C. Williams, N. Hong, M. Julian, S. Borg, and H. J. Kim, "Tunable mid-wave infrared Fabry-Perot bandpass filters using phase-change GeSbTe," Opt. Express **28**(7), 10583–10594 (2020).
21. M. Rudé, V. Mkhitaryan, A. E. Cetin, T. A. Miller, A. Carrilero, S. Wall, F. J. G. de Abajo, H. Altug, and V. Pruneri, "Ultrafast and Broadband Tuning of Resonant Optical Nanostructures Using Phase-Change Materials," Adv. Opt. Mater. **4**(7), 1060–1066 (2016).
22. Z. Zhu, P.G. Evans, R.F. Haglund Jr., and J.G. Valentine, "Dynamically Reconfigurable Metadevice Employing Nanostructured Phase-Change Materials," Nano Lett. **17**(8), 4881–4885 (2017).
23. V. K. Mkhitaryan, D. S. Ghosh, M. Rudé, J. Canet-Ferrer, R. A. Maniyara, K. K. Gopalan, and V. Pruneri, "Tunable Complete Optical Absorption in Multilayer Structures Including $Ge_2Sb_2Te_5$ without Lithographic Patterns," Adv. Opt. Mater. **5**(1), 1600452 (2017).
24. X. Sun, R. Hong, H. Hou, Z. Fan, and J. Shao, "Thickness dependence of structure and optical properties of silver films deposited by magnetron sputtering," Thin Solid Films **515**(17), 6962–6966 (2007).
25. L. A. Pettersson, L. S. Roman, and O. Inganäs, "Modeling photocurrent action spectra of photovoltaic devices based on organic thin films," J. Appl. Phys. **86**(1), 487–496 (1999).
26. Q. He, Z. Li, J. Peng, Y. Deng, B. Zeng, W. Zhou, and X. Miao, "Continuous controllable amorphization ratio of nanoscale phase change memory cells," Appl. Phys. Lett. **104**(22), 223502 (2014).
27. T. Matsunaga, J. Akola, S. Kohara, T. Honma, K. Kobayashi, E. Ikenaga, R. O. Jones, N. Yamada, M. Takata, and R. Kojima, "From local structure to nanosecond recrystallization dynamics in AgInSbTe phase-change materials," Nat. Mater. **10**(2), 129–134 (2011).
28. G. Rodriguez-Hernandez, P. Hosseini, C. Ríos, C. D. Wright, and H. Bhaskaran, "Mixed-mode electro-optical operation of Ge2Sb2Te5 nanoscale crossbar devices," Adv. Electron. Mater. **3**(8), 1700079 (2017).
29. M. Ye, L. Sun, X. Hu, B. Shi, B. Zeng, L. Wang, J. Zhao, S. Yang, R. Tai, H.-J. Fecht, J.-Z. Jiang, and D.-X. Zhang, "Angle-insensitive plasmonic color filters with randomly distributed silver nanodisks," Opt. Lett. **40**(21), 4979 (2015).
30. P. Ji, C.-S. Park, S. Gao, S.-S. Lee, and D.-Y. Choi, "Angle-tolerant linear variable color filter based on a tapered etalon," Opt. Express **25**(3), 2153 (2017).
31. B. Broughton, L. Bandhu, C. Talagrand, S. Garcia-Castillo, M. Yang, H. Bhaskaran, and P. Hosseini, Dig. Tech. Pap. - Soc. Inf. Disp. Int. Symp. 2017, 48, 546.
32. C. Talagrand, G. Triggs, L. Bandhu, S. Garcia-Castillo, B. Broughton, H. Bhaskaran, and P. Hosseini, J. Soc. Inf. Disp. 2018.